

CLOSED LOOP ORGANIC VAPOR WIND TUNNEL CLOWT: COMMISSIONING AND OPERATIONAL EXPERIENCE

Felix Reinker^{1*}, Eugeny Y. Kenig², Stefan aus der Wiesche¹

¹ Muenster University of Applied Sciences,
Department of Mechanical Engineering,
48565 Steinfurt, Germany
f.reinker@fh-muenster.de
wiesche@fh-muenster.de

² Paderborn University, Chair of Fluid Process Engineering,
33098 Paderborn, Germany
eugeny.kenig@uni-paderborn.de

* Corresponding Author

ABSTRACT

In this contribution, the commissioning of the Closed Loop Organic Vapor Wind Tunnel (CLOWT) is discussed and first operational experience of this test facility is presented. The paper comprises four parts. In the first part, the low-speed aerodynamics of CLOWT, based on measurements with Constant Temperature Anemometry (CTA) and Pitot-Static Tubes, is analyzed. Due to the fact that CLOWT acts as a pressure vessel system, leakage issues are of fundamental importance for this facility. For this reason, in the second part, both static leakage tests (without shaft rotation) and dynamic leakage tests focusing on the shaft sealing are discussed. CLOWT follows the concept of a continuous running mode. Therefore, in the third part, the thermal longterm behavior is considered, while time-dependent temperature and pressure measurements inside the test section are shown. In the last part, the compressor performance is presented. Based on the commissioning and first operational experience, an outlook for future experiments with organic fluids is given.

1. INTRODUCTION

The Organic Rankine Cycle (ORC) is a sustainable heat conversion technology which offers the possibility of reducing the fossil fuel demand by utilizing waste heat and renewables. The cycle principle is based on the Rankine cycle performed with organic working fluids. In contrast to steam and air, the thermodynamic behavior of nearly all organic fluids is associated with strong real-gas effects and a low speed of sound which significantly complicates expanders design [1, 2, 3, 4]. Nonideal gas behavior is described by the compressibility factor Z [5], while real gas effects appear for $Z < 1$. Steam applications also involve real gas effects. The perfect vapor assumption by Traupel can be used to account for real gas effects in steam applications [6, 7]. In case of organic fluids, this assumption is not applicable, because the compressibility factor also depends on factors other than entropy [8].

Computational Fluid Dynamic (CFD) tools are currently widely utilized to optimize the expansion processes in terms of machine performance. On the one hand, the accuracy of the thermodynamic models, describing the thermophysical properties of a substance strongly affects the calculation results. On the other hand, the computation of organic vapor flows in the so-called dense gas regime, close to the vapor saturation curve, still represents a major difficulty. To account for these uncertainties, validation studies based on experiments are needed [4, 9]. However, experimentally based validation studies are still hardly available because of the special test rig design which is required for organic fluids. The design of these test rigs is rather challenging in respect to both technical issues and investment costs [10]. Nevertheless, a few test rigs have been constructed in the last few years. A detailed discussion on these test

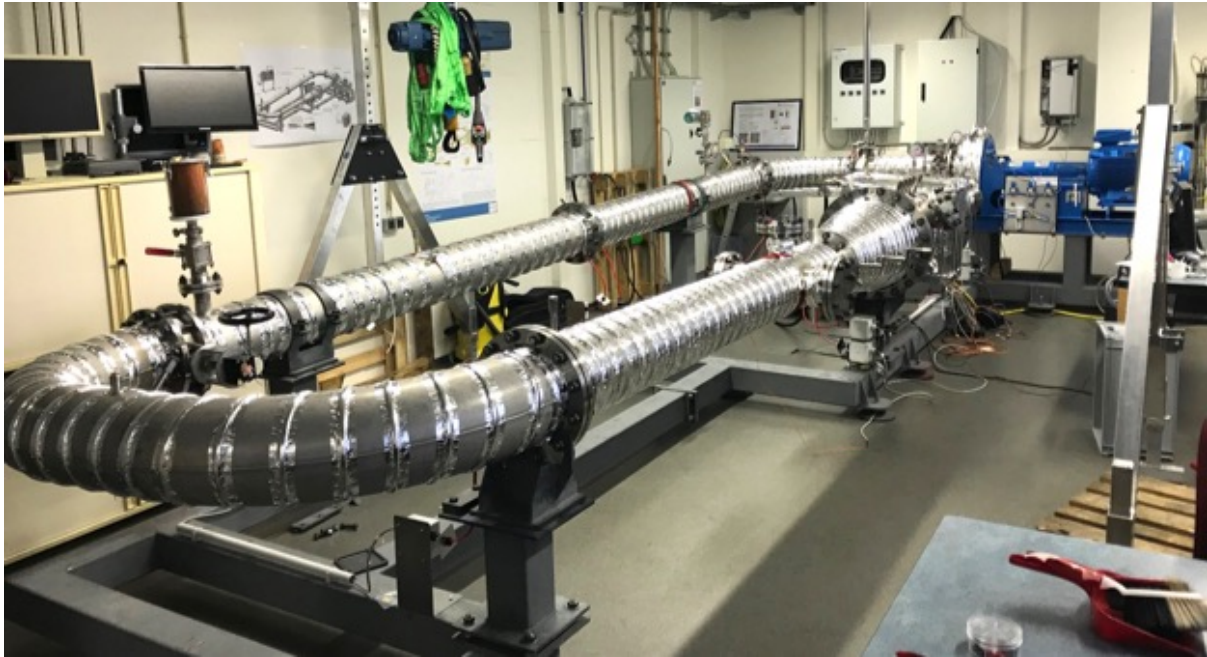


Figure 1: Photo of the Closed Loop Organic Vapor Wind Tunnel (CLOWT) taken during the commissioning. Afterwards CLOWT was insulated.

rigs for organic vapors is given in [11]. Figure 1 shows a photo of CLOWT. It follows the concept of a closed-loop continuously running wind tunnel and it is designed for operation with the perfluorinated ketone Novec™ 649 at elevated pressure and temperature levels [12]. The modular design of CLOWT permits investigations on blowers, small axial test turbines, nozzle flows or transonic flows past test objects. More details on the design of CLOWT can be found in [8, 11, 13]

This contribution discusses the commissioning of and the first operational experience obtained with CLOWT.

2. LOW-SPEED AERODYNAMICS OF CLOWT

Test rigs for the investigation of organic vapor flows can exploit different design concepts. On the one hand, there are intermittent facilities like TROVA [14]. On the other hand, there are continuously running facilities like ORCHID [15] or CLOWT, which is presented here.

CLOWT follows the concept of a continuous running facility and is based on the principles of a closed-gas cycle. In addition to pressure vessel design constraints, major attention was given to classical wind tunnel design guidelines. This was necessary because of a critical wide-angle diffuser just after the compressor and a contraction zone, which had to be manufactured in a conical piecewise manner, because of pressure vessel design constraints.

For this reason, the low-speed aerodynamics of CLOWT, including the critical components mentioned above, have to be investigated. The detection of velocity fluctuations inside the diffuser, settling-chamber and test section were performed by one-dimensional CTA measurements. The measurements were performed with air, instead of Novec™ 649, as working fluid. This was possible, because all of the investigated components show low speed aerodynamics ($Ma < 0.3$). Nevertheless, CTA measurements with Novec™ 649 require dedicated probe calibration which is excessively expensive. Additionally, the velocity profile inside the test section was determined by means of a Pitot-Static Tube, mounted on an adjustable linear bearing. Figure 2 shows a sketch of the flow path, including diffuser, settling chamber, 1st contraction and test section. CTA measurements were taken at three different positions. The first position (I) is placed at the outlet of the diffuser, just before the flow enters the finned heat exchanger in the settling chamber. The second position (II) is placed at the outlet of the settling chamber, just before the flow enters the 1st contraction. The third position (III) is finally placed at the entrance of the test

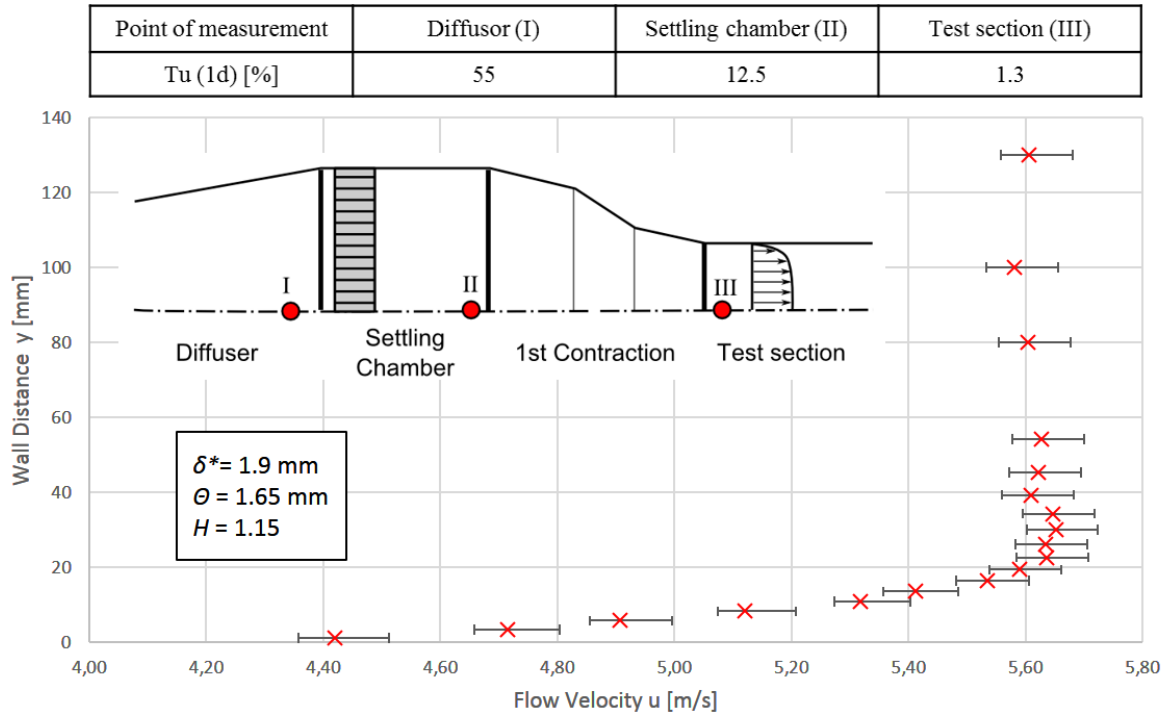


Figure 2: Wall distance as function of the flow velocity in the entrance of the test section, including error bars for the flow velocity. The sketch shows the three CTA measurements points (I, II, and III) along the flow path as well as the measurement position of the velocity profile. Corresponding values for Tu are given in the table above.

section, just after the outlet of the 1st contraction. The table on top of Figure 2 gives the corresponding values of the one dimensional turbulence intensity, Tu . The diffuser shows a very high turbulence intensity of 55%. This value was expected, because there were no turbulence screens installed inside of the wide angle diffuser, leading to flow separation at the walls. Although the settling chamber was not yet equipped with turbulence screens and flow straighteners, the turbulence intensity was reduced to 12.5%. The finned heat exchanger seems to act like a slight flow straightener. The third, most important, measurement position in the test section shows a turbulence intensity of 1.3%, which is fairly acceptable in view of the fact that the settling chamber was nearly empty (no screens).

Figure 2 also shows the velocity profile in the entrance of the test section. The analysis of the velocity values lead to a displacement thickness of $\delta^* = 1.9$ mm and a momentum thickness of $\Theta = 1.65$ mm. The corresponding shape factor, which is the ratio of δ^* to Θ , is $H = 1.15$. This value is in a reasonable range for a turbulent pipe flow [16].

3. LEAKAGE TESTS

Due to the fact that CLOWT acts as a pressure vessel system, leakage issues are of fundamental importance for this facility. Figure 3 B) shows the components of the shaft sealing of the compressor. Sealing of rotating shafts is a standard task for manufacturers of fans and compressors, but sealing of an organic vapor in combination with shaft rotation is very difficult. For this reason, the cartridge multiple dynamic lip seal system used for CLOWT is a custom product (for details see [11]).

To investigate the leakage rate of CLOWT, the so-called pressure drop test was applied. In the first step, the pressure vessel system was brought up on a higher pressure level (e.g. 5 bar). After a temperature settling time of several hours, the actual mass m_i of working fluid (in this case air) was determined by

$$m_i = \frac{p_i \cdot V_0}{R \cdot T_i} \quad (1)$$

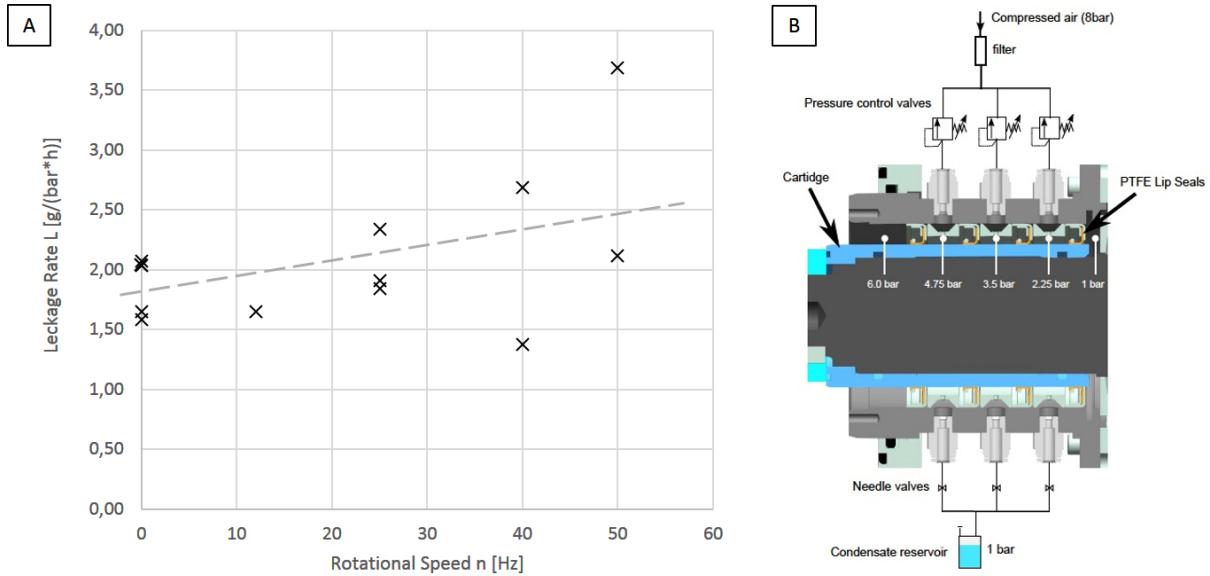


Figure 3: A) Leakage rate of the pressure vessel system as function of the rotational speed of the compressor at different pressure levels, B) Schematic drawing of the cartridge multiple dynamic lip seal system of the radial compressor

Such a determination was repeated after one hour of "leakage time" to finally calculate the static leakage rate L (without shaft rotation) by

$$L = \frac{\Delta m}{\bar{p} \cdot \Delta t}. \quad (2)$$

In the next step, the compressor was started and set on a rotational speed n . After one hour, the shaft rotation was stopped and the actual mass of working fluid was determined again to calculate the dynamic leakage rate of the operational mode. Figure 3 A) shows the leakage rates of CLOWT for different pressure levels (1-4 bar). The static leakage rate of about $2.0 \frac{\text{g}}{\text{bar}\cdot\text{h}}$ is very small. A slight dependence of the leakage rate L on the rotational speed n is apparent. This relation was expected. Nevertheless, the leakage values are reasonable.

4. THERMAL LONGTERM BEHAVIOR

CLOWT follows the concept of a continuous running mode. For this reason, the achievement of steady-state conditions inside of the test section is of major interest. The thermal longterm behavior of CLOWT, including time-dependent temperature and pressure measurements, are presented in this section.

Prior to the operation of CLOWT, filling and evaporation procedures have to be performed. These procedures are illustrated by means of a measurement data set in Figure 4. Figure 4 A) shows the time course of temperature T , whereas Figure 4 B) reveals the time course of pressure p . First, the pressure vessel system is evacuated ($t = 0 - 500$ s). Next, the suction line is opened and NovecTM 649 is filled to the wind tunnel ($t = 500 - 600$ s). The rapid decrease of temperature also indicates the start of the filling. In the next step, the heating system is started and the working fluid is evaporated. The logarithmic growth of temperature indicates the evaporation of the two-phase system. At $t = 6100$ s, the compressor is started and set on a rotational speed of $n = 20$ Hz, accelerating the evaporation process. At $t = 6500$ s, the rapid pressure rise ends, which indicates that the whole liquid phase is evaporated and NovecTM 649 remains in the superheated state. CLOWT is now ready for operation.

In the following, an exemplary operating point with NovecTM 649 is discussed in terms of steady-state conditions. Figure 5 shows a time period of $\Delta t = 400$ s. Figure 5 A) shows the flow rate \dot{V} , which is determined by an averaging pitot tube in the return. The very small fluctuations are due to the mea-

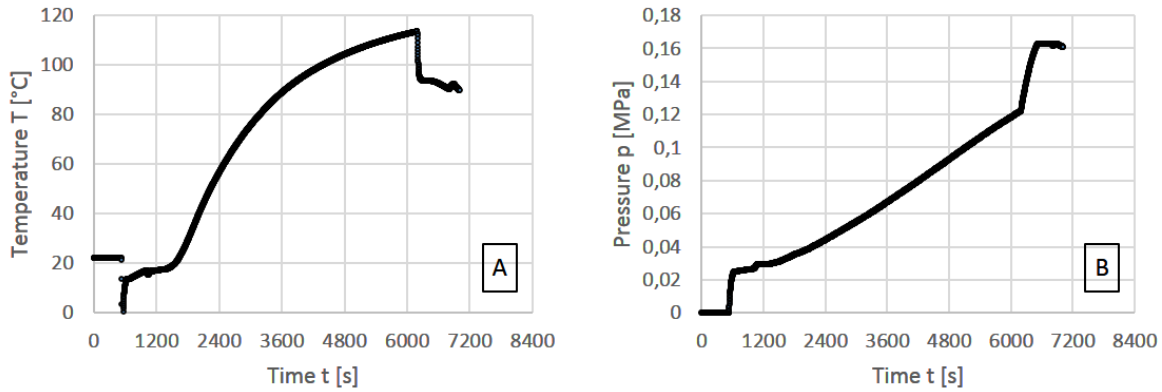


Figure 4: A) Time course of temperature near the filling valve during the filling and evaporation process, B) Time course of the static pressure during the filling and heating process

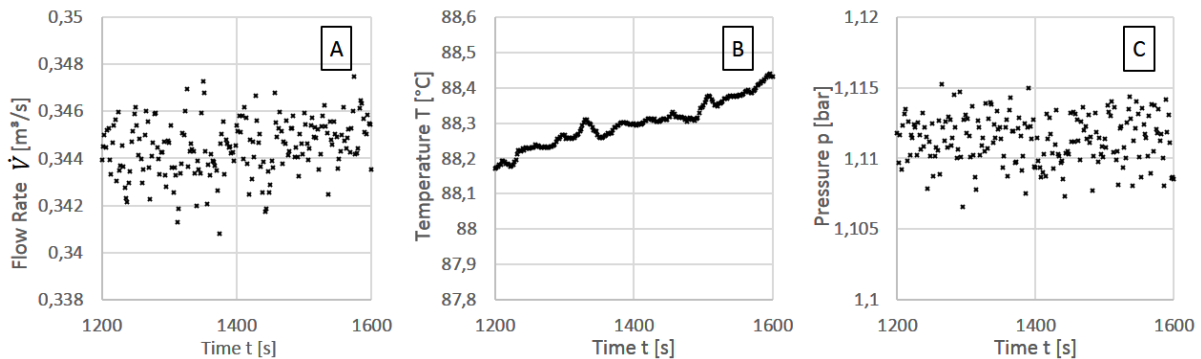


Figure 5: A) Fluctuations of the flow rate within 400 seconds, B) Fluctuations of temperature in the test section within 400 seconds, C) Fluctuations of the static pressure in the test section within 400 seconds

surement accuracy of 1%. Figure 5 B) shows a small drift in temperature T , approximately equal to $\Delta T = 0.2$ K. The measurement accuracy of the used Resistance Temperature Detector (RTD) of class 1/10 DIN B is smaller than 0.1 K. Further, Figure 5 C) demonstrates the corresponding pressure level p . The fluctuations are also very small and remain in the measurement accuracy of 0.1% of the pressure transducer. Thanks to the weak dependency of pressure on temperature in the superheated region, the pressure remains nearly constant.

As a result of this measurements one can conclude that CLOWT passed the examination on stationarity for a measurement time of about $\Delta t = 400$ s. This time slot should be long enough for most of the flow investigations in the test section.

5. COMPRESSOR PERFORMANCE

The compressor performance of a wind tunnel is also very important for setting the final test section operation conditions. Prior to the operation of CLOWT with NovecTM 649, the wind tunnel was operated with air as working fluid. These measurements provided valuable experience, e.g. the low speed aerodynamics of Figure 2 or the leakage rates of Figure 3. These measurements were performed through the compressors characteristic curve determination. In order to simplify the interpretation of the compressor head at different density levels, the specific work h was chosen. Figure 6 shows the characteristic compressor curves for air and for NovecTM 649. Fortunately the design operation point specifications of the manufacturer are matched for both fluids at a flow rate of about $\dot{V} = 0.3 \frac{\text{m}^3}{\text{s}}$. Furthermore, the specific work h for air matches for the whole working area with the specifications. However, there are deviations

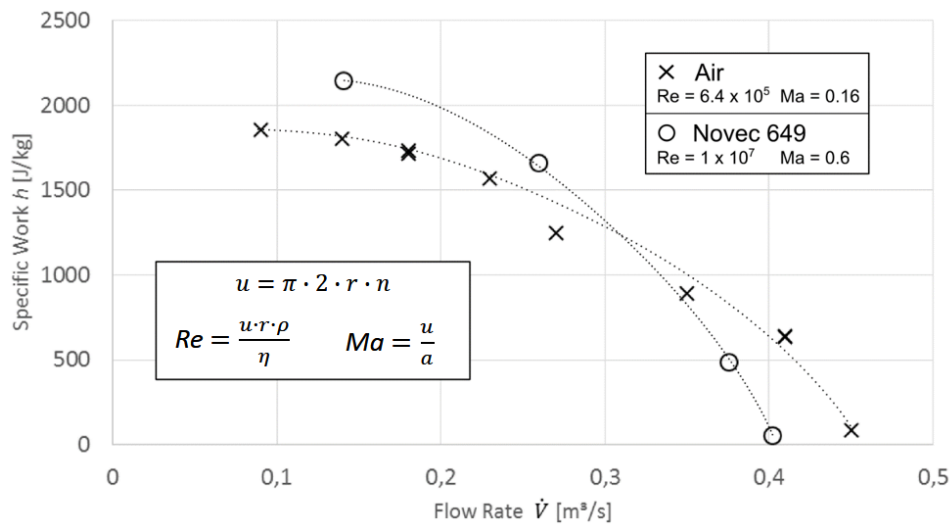


Figure 6: Specific work as function of flow rate for air and Novec™ 649 as working fluids. Relevant Reynolds and Mach numbers of the experiments with calculation method are shown in boxes.

between air and Novec™ 649 in off-design conditions apparent. Given the fact that Novec™ 649 shows a strong real gas behavior and a very low speed of sound, the deviations at higher flow rates are reasonable. For this reason the relevant Reynolds and Mach numbers were calculated for both fluids (see boxes in Fig. 6). The calculations are based on the circumferential speed u and the radius r of the radial impeller, and on the speed of sound a , which significantly differs between air and Novec™ 649. The deviations of h for $\dot{V} > 0.3 \frac{\text{m}^3}{\text{s}}$ appear reasonable regarding the relative high Mach number ($Ma = 0.6$) of Novec™ 649 at the impeller outlet. Nevertheless, a more detailed investigation on the compressor performance is necessary to identify the reason for the deviations in specific work h for air and Novec™ 649. On the one hand, the reason for the positive deviations of Novec™ 649 at flow rates $\dot{V} < 0.3 \frac{\text{m}^3}{\text{s}}$ is not clarified yet, but on the other hand, the exceeding of the expectations is helpful in terms of reaching the test section design point.

6. CONCLUSION AND OUTLOOK

The commissioning of CLOWT and first time operational experience with Novec™ 649 as working fluid in a wind tunnel are presented in this contribution. The low speed aerodynamics of the critical components (diffuser, settling chamber, 1st contraction, and test section) were investigated by terms of CTA measurements and pitot static tubes. The results are reasonable in view of the fact there were no screens and flow straighteners installed. Leakage of CLOWT was investigated using the so-called pressure drop test. The results with air are satisfactory. Prior to the the investigation of the thermal longterm behavior of CLOWT, the filling process of CLOWT was studied, based on experimental measurements. The analysis of the thermal longterm behavior in the test section shows that CLOWT is ready for steady-state measurements within $\Delta t = 400 \text{ s}$. Finally the experimental data of the compressor performance curves with both substances air and Novec™ 649 are shown. The design operation point specifications of the manufacturer are matched for both fluids. The specific work with Novec™ 649 below the design point flow rate even exceeds the expectations.

One of the next steps will be the determination of the turbulence intensity of Novec™ 649 inside the test section using the flow past a sphere. Furthermore, the construction of a second contraction zone, followed by a test bench for the investigation of pressure distributions on airfoils and turbine blades, is ongoing work.

NOMENCLATURE

a	Speed of sound	$[\frac{m}{s}]$
CTA	Constant temperature anemometry	
H	Shape factor	$[-]$
h	Specific work	$[\frac{J}{kg}]$
L	Leakage Rate	$[\frac{g}{bar \cdot h}]$
m	Filling mass	$[kg]$
Ma	Mach number	$[-]$
n	Rotational speed	$[Hz]$
p	Pressure	$[bar]$
R	Specific gas constant	$[\frac{J}{mol \cdot K}]$
r	Radius (radial impeller)	$[m]$
T	Temperature	$[^{\circ}C]$
t	Time	$[s]$
Tu	Turbulence intensity	$[\%]$
u	Circumferential speed (radial impeller)	$[\frac{m}{s}]$
V	Volume	$[m^3]$
\dot{V}	Flow rate	$[\frac{m^3}{s}]$
Z	Compressibility factor	$[-]$

Greek Symbols

δ^*	Displacement thickness	$[mm]$
ρ	Density	$[\frac{kg}{m^3}]$
Θ	Momentum thickness	$[mm]$

Subscript

0	stagnation state
i	running index

REFERENCES

- [1] Invernizzi, C. M., 2013. *Closed Power Cycles*, Vol. 11 of *Lecture notes in energy*. Springer, London, UK.
- [2] Colonna, P., Casati, E., Trapp, C., Mathijssen, T., Larjola, J., Turunen-Saaresti, T., and Uusitalo, A., 2015. “Organic rankine cycle power systems: From the concept to current technology, applications, and an outlook to the future”. *ASME Journal of Engineering for Gas Turbines and Power*, **137**(10), p. 100801.
- [3] Macchi, E., and Astolfi, M., 2017. *Organic rankine cycle (ORC) power systems: Technologies and applications*, Vol. number 107 of *Woodhead Publishing series in energy*.
- [4] Merle, X., and Cinnella, P., 2014. “Bayesian quantification of thermodynamic uncertainties in dense gas flows”. *Reliability Engineering & System Safety*, **134**, pp. 305–323.
- [5] Colonna, P., Rebay, S., Harnick, J., and Guardone, A., 2006. “Real-gas effects in orc turbine flow simulations: Influence of thermodynamic models on flow fields and performance parameters”. *ECCOMAS CFD 2006*.
- [6] Traupel, W., 1952. “Zur dynamik realer gase”. *Forschung auf dem Gebiete des Ingenieurwesens*, **18**(1), pp. 3–9.
- [7] Traupel, W., 2001. *Thermische Turbomaschinen*, 4. aufl. ed. Klassiker der Technik. Springer, Berlin.
- [8] Reinker, F., Hasselmann, K., aus der Wiesche, S., and Kenig, E. Y., 2015. “Thermodynamics and fluid mechanics of a closed blade cascade wind tunnel for organic vapors”. *ASME Journal of Engineering for Gas Turbines and Power*, **138**(5), p. 052601.
- [9] Congedo, P. M., Cinnella, P., and Corre, C., 2009. “Shape optimization for dense gas flows in turbine cascades”. *Shape Optimization for Dense Gas Flows in Turbine Cascades*. In: *Deconinck H., Dick E. (eds) Computational Fluid Dynamics 2006*. Springer, pp. 555–560.
- [10] Spinelli, A., Dossena, V., Gaetani, P., Osnaghi, C., and Colombo, D., 2010. “Design of a test rig for organic vapors”. *Proceedings of ASME Turbo Expo 2010*, pp. 109–120.
- [11] Reinker, F., Kenig, E. Y., and aus der Wiesche, S., 2018. “Clowt: A multifunctional test facility for the investigation of organic vapor flows”. *ASME 2018 5th Joint US-European Fluids Engineering Division Summer Meeting*, **2018**, p. V002T14A004.
- [12] Tuma, P. E., 2008. “Fluoroketone c2f5c(o)cf(cf3)2 as a heat transfer fluid for passive pumped 2-phase applications”. *2008 Twenty-fourth Annual IEEE Semiconductor*, pp. 173–179.
- [13] Reinker, F., Kenig, E. Y., Passmann, M., and aus der Wiesche, S., 2017. “Closed loop organic wind tunnel (clowt): Design, components and control system”. *Energy Procedia*, **129**, pp. 200–207.
- [14] Spinelli, A., Pini, M., Dossena, V., Gaetani, P., and Casella, F., 2013. “Design, simulation, and construction of a test rig for organic vapors”. *ASME Journal of Engineering for Gas Turbines and Power*, **135**(4).
- [15] Head, A. J., de Servi, C., Casati, E., Pini, M., and Colonna, P., 2016. “Preliminary design of the orchid: A facility for studying non-ideal compressible fluid dynamics and testing orc expanders”. *ASME Turbo Expo 2016: Turbomachinery Technical Conference and Exposition*, p. V003T25A001.
- [16] Schlichting, H., 1979. *Boundary-layer theory*, 7. ed. ed. MacGraw-Hill series in mechanical engineering. MacGraw-Hill, New York and Düsseldorf u.a.